Electronic and Magnetic Properties of Zigzag Graphene Nanoribbons on the (111) Surface of Cu, Ag, and Au

Yan Li,[1] Wei Zhang,[1] Markus Morgenstern,[2] and Riccardo Mazzarello[1,*]

[1]*Institute for Theoretical Solid State Physics and JARA, RWTH Aachen University, D-52074 Aachen, Germany*
[2]*II. Physikalisches Institut B and JARA-FIT, RWTH Aachen University, D-52074 Aachen, Germany*

(Received 2 October 2012; published 24 May 2013)

We carry out an *ab initio* study of the structural, electronic, and magnetic properties of zigzag graphene nanoribbons on Cu(111), Ag(111), and Au(111). Both, H-free and H-terminated nanoribbons are considered revealing that the nanoribbons invariably possess edge states when deposited on these surfaces. In spite of this, they do not exhibit a significant magnetization at the edge, with the exception of H-terminated nanoribbons on Au(111), whose zero-temperature magnetic properties are comparable to those of free-standing nanoribbons. These results are explained by the different hybridization between the graphene $2p$ orbitals and those of the substrates and, for some models, also by the charge transfer between the surface and the nanoribbon. Interestingly, H-free nanoribbons on Au(111) and Ag(111) exhibit two main peaks in the local density of states around the Fermi energy, which originate from different states and, thus, do not indicate edge magnetism.

DOI: 10.1103/PhysRevLett.110.216804 PACS numbers: 73.22.Pr, 71.15.Mb, 75.70.Ak

Graphene, with its remarkable electronic and transport properties [1], in particular, a high mobility at room temperature for supported samples [2,3], is a promising material for applications in information technology. While perfect monolayer graphene has a gapless spectrum prohibiting standard transistor applications, nanostructuring can induce the required band gap. Recent efforts focused on quasi one-dimensional graphene nanoribbons (GNRs) [4–7] and zero-dimensional graphene quantum dots (GQDs) [8–10] and, indeed, revealed a transport gap, e.g., for GNRs with widths below 10 nm. Theoretically, unsupported GNRs and GQDs with zigzag edge geometry possess spin polarized edge states with ferromagnetic order along the edge [11–13]. Several experimental studies provide direct [10,14–16] or indirect [17] evidence for the presence of the edge states also in supported GNRs, albeit without probing its magnetism. Such edge states might be exploited for a multitude of spintronics applications [4,18–20], but so far it is unclear if the edge states contribute to the measured transport properties of nanostructures at all [21]. Thus, it is important to elucidate the role of the substrate and of edge termination. Recently, several groups including us investigated *in situ* prepared GQDs with exclusive zigzag edges, which are supported by Ir(111) [22–28]. In particular, we revealed the absence of edge states by a combined density functional theory (DFT) and scanning tunneling microscopy study [29]. Our finding was explained by a hybridization of the graphene π orbitals with an Ir $5d_{z^2}$ surface state at E_F, which gradually decreases in strength from the edge towards the center of the GQD and, thus, prohibits a simple shift of the edge state towards the interior of the GQD [29]. In contrast, scanning tunneling microscopy studies of Tao *et al.* [16] provided convincing evidence for the presence of edge states in GNRs chemically prepared from carbon nanotubes by so-called unzipping [30] and deposited on Au(111). A peak or a double-peak close to E_F was observed in the local density of states close to the edge with a peak distance ΔE scaling inversely with the width of the GNR ($\Delta E \sim 20$–50 meV for widths of 8–20 nm [16]). The double peak was present for chiral angles θ up to 16.1° with respect to the zigzag direction and was ascribed to an antiferromagnetic coupling between opposite edges [16,31], as further evidenced by comparison with results from a Hubbard model Hamiltonian [16]. Here, we present a more realistic description of this system using DFT and including the Au(111) surface. Large models enable us to study GNRs of close to realistic widths and to correctly describe the lattice mismatch between graphene and Au(111). We also investigate GNRs deposited on Cu(111) and Ag(111). For all the substrates, we consider both H-free and singly H-terminated GNRs. For H-free GNRs on Au(111), we consider the chiral angles $\theta = 0°$ and 5°, while only perfect zigzag GNRs are studied for the other systems. All the GNRs studied exhibit edge states, but the interaction with the substrate strongly depends on whether the GNR is H terminated or not and, to a lesser extent, on the type of substrate. It turns out that the edge states are magnetic only when H terminated and deposited on Au(111). Interestingly, the nonmagnetic H-free GNR on Au(111) exhibits a double peak around E_F, with splitting $\Delta E \sim 500$ meV, but the two peaks originate from a hybridization of Au d orbitals with the C dangling-bond orbitals and the edge state, respectively, and not from a magnetic splitting of the edge state.

We consider GNRs with zigzag edges and a width of 8 graphene unit cells. We employ different supercells in order to account for (i) the lattice mismatch between graphene and the (111) surfaces of Ag and Au, and

(ii) chiral angles. Here, we describe the models having $\theta = 0°$ (the model with finite θ is discussed in the Supplemental Material [32]). For Ag and Au a supercell with a size parallel to the GNR six times as large as the unit cell of the (111) surface was used. For Cu, an extremely large supercell would be required to account for the mismatch, making the calculations unfeasible. Therefore, we use a compressed (about 3.8%) Cu lattice to make graphene and Cu(111) commensurate. A four-layer slab was used for Ag and Au surfaces, whereas the use of a smaller supercell for Cu (in the direction parallel to the GNR) enabled us to employ thicker slabs containing up to 12 layers. The latter calculations showed that 4-layer slabs are sufficient to describe the interaction between the GNR and the Cu surface (see Supplemental Material [32]), making us confident that the same holds true for Ag and Au substrates.

The structural optimization and the calculation of the electronic and magnetic properties were carried out using the plane-wave package QUANTUM-ESPRESSO [33]. We employed gradient-corrected exchange correlation functionals [34] and semiempirical Grimme corrections (DFT-D2) to describe van der Waals interactions [35]. Additional computational details are provided in the Supplemental Material [32].

In the first part of the Letter, we present our results about the GNRs on Au(111). Ag and Cu substrates are discussed in the second part and in the Supplement Material [32]. Upon DFT relaxation, the H-free GNR with $\theta = 0°$ on Au(111) bends considerably: the distance between C atoms and the surface is much shorter at the GNR edge than in the interior of the ribbon [Fig. 1(a)]. The maximum distance between C atoms and the Au (as well as Cu and Ag) surface at the center of the GNR and the minimum distance at the edge are shown in Table I. A small corrugation (about 0.17 Å) along the GNR edges in accordance with the common periodicity of the two lattices is observed. In particular, 4 edge C atoms out of 7 are in a quasi on-top configuration, whereas the remaining edge atoms are in a quasi bridge or hollow configuration. In the following, the z axis will be taken perpendicular to the surface and the x axis will be taken parallel to the GNR. Since the GNR is not parallel to the surface at the edge, the orbitals of C forming edge states are linear combinations of $2p_z$ and $2p_y$ orbitals. For the same reason, the dangling-bond orbitals of the edge C atoms of the H-free GNR (which form σ bonds with Au atoms upon deposition on the surface, see below) are also combinations of these orbitals. In Fig. 1(b) the $(p_y + p_z)$ projected density of states (PDOS) of a C atom in the middle part of the GNR and the PDOS of the $5d$ states of an Au atom located beneath are shown: the contribution of the PDOS of the d states of Au near E_F is very small and the interaction between the two atoms is basically negligible. On the other hand, a comparison of the PDOS of the d states of several Au atoms starting from an

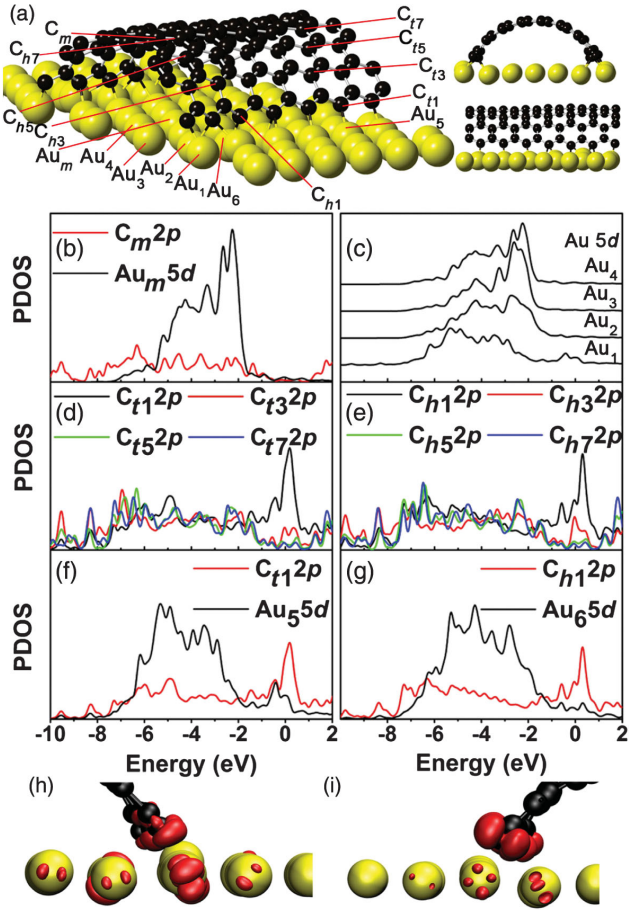

FIG. 1 (color). Structural and electronic properties of a H-free GNR on Au(111). (a) Topography of the relaxed model. For the sake of clarity, only the top Au layer is shown. C and Au atoms are labeled by numbers indicating different chemical environments and used in (b)–(g). The top and hollow adsorption sites of the edge C atoms are denoted with the subscripts "t" and "h" respectively. (b) $(p_y + p_z)$-PDOS of a C atom (C_m) in the middle part of the GNR and PDOS of the d states of an Au atom (Au_m) located beneath. (c) PDOS of d states of several Au atoms starting from an atom below the edge of the GNR (Au_1) towards an atom below the centre of the GNR (Au_4). (d), (e) $(p_y + p_z)$-PDOS of C atoms at the center of the on-top (d) and hollow (e) region, in increasing distance from the edges; row 1 denotes the edge row. (f), (g) $(p_y + p_z)$-PDOS of an edge C atom at on-top site, C_{t1} (f), and at hollow site, C_{h1} (g), and PDOS of the d states of the nearest neighbor Au atom (Au_5 and Au_6 respectively). (h), (i) Plots of a charge isosurface of a state contributing to the peak at -0.2 eV below E_F (h) and at 0.3 eV above E_F (i).

Au atom below the edge of the GNR towards an Au atom below the center [Fig. 1(c)] shows that, at the edge, the PDOS displays some peaks near E_F. Also, the $(p_y + p_z)$ PDOS of the edge C atoms [Figs. 1(d) and 1(e)] exhibit two main peaks near E_F. To shed light on the interaction between edge C atoms and Au atoms, it is useful to compare the respective PDOS at on-top sites [Fig. 1(f)] and hollow sites [Fig. 1(g)]. The $(p_y + p_z)$ PDOS of a

TABLE I. Minimum distance between the edge C atoms of the GNR and the atoms of the relevant (111) surface and maximum distance between the center of the GNR and the surface. Distances are in Angstrom.

	H-free GNR		H-terminated GNR	
	min	max	min	max
Cu	1.96	3.31	2.37	3.06
Ag	2.18	5.61	2.69	3.16
Au	2.12	5.86	3.31	3.64

C atom at an on-top site displays two peaks at -0.2 eV below and 0.3 eV above E_F, respectively. Inspection of the PDOS of the nearest neighbor Au $5d$ orbitals indicates that a strong hybridization between these states and C states occurs. In particular, a relatively high peak below E_F is present, in correspondence with the small peak of the C p states, whereas a less pronounced peak is found right above E_F, corresponding to the second, large peak of the C p PDOS. In the hollow case, two peaks are present in the PDOS of C p states and Au d states near E_F as well. The plots of charge isosurfaces of two states contributing to said two peaks in the PDOS of C p orbitals [Figs. 1(h) and 1(i)] show that they have a different origin, in that the one above E_F is due to the π edge state of the GNR, whereas the one below E_F is due to states originating from σ bonding between C and Au atoms. More precisely, the latter peak corresponds to antibonding p-d states, whereas the corresponding bonding states have much lower energies (about -5 eV below E_F, see Supplemental Material [32]). In the on-top case, the $5d_{z^2}$ and $5d_{yz}$ orbitals of the Au mostly contribute to the bonding with C p states; in the hollow case, $5d_{zx}$ orbitals contribute as well. Au $6s$ and $6p$ orbitals do not play an important role in this bonding. Since the antibonding σ states have lower energies than the edge states, the latter states are mostly unoccupied and no significant edge magnetism occurs (less than $3 \times 10^{-3} \mu_B$ per edge C atom).

The model of the GNR with $\theta = 5°$ also bends considerably and exhibits essentially nonmagnetic edge states for similar reasons (see Supplemental Material [32]).

Next, we consider H-terminated GNRs on Au(111), a system that has recently been prepared experimentally [30,36,37]. In this case, the interaction between the GNR and the surface is weak. There exist two adsorption configurations: in the lower-energy one, the adsorption site of the edge C atoms changes gradually from on top to bridge along the edge, and the minimum distance between the edge C atoms and the surface is 3.31 Å (see Table I). The GNR is slightly bent, as evident from Figs. 2(a) and 2(b). In the second configuration, the adsorption site of the edge C atoms changes from hollow to (quasi) bridge: this structure is also magnetic and is discussed in the Supplemental Material [32]. The electronic properties of the GNR are weakly affected by the presence of the substrate: the GNR displays a magnetic edge state with antiferromagnetic

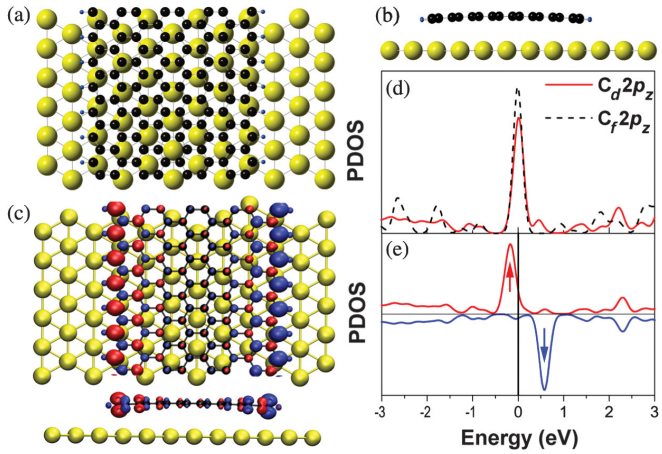

FIG. 2 (color). Structural and electronic properties of a H-terminated GNR on Au(111). (a), (b) Top and side view of the relaxed model. Only the top Au layer is shown. (c) Top and side view of an isovalue surface of the edge state spin density of the deposited GNR. The system has antiferromagnetic order across the GNR. The red (blue) surface indicates spin up (down) density. (d) Non-spin-polarized PDOS of the $2p_z$ orbitals of an edge C atom of the deposited GNR (C_d). The corresponding PDOS of the edge C atom of the free-standing GNR (C_F) is also shown for comparison. (e) Spin-polarized PDOS of the $2p_z$ orbitals of a C atom at the left edge of the magnetized GNR shown in (c).

coupling between the edges and the magnetization per edge C atom is about $0.22 \mu_B$ (comparable to the value obtained for free-standing GNRs using equivalent k-point meshes, see Supplemental Material [32]). An isovalue surface of the edge state spin density is shown in Fig. 2(c), whereas the spin-unpolarized and spin-polarized PDOS of the $2p_z$ orbitals of edge C atoms are shown in Figs. 2(d) and 2(e) respectively. The energy splitting between spin majority and minority $2p_z$ peaks on an edge is about 0.7 eV [Fig. 2(e)].

Since the edges of the GNRs investigated experimentally in Ref. [16] exhibit a pronounced edge curvature, they resemble the H-free case of our calculation. A comparison of the experimentally observed peak splitting with the calculated one is tempting, although the experimental GNR width of 8 to 20 nm is much larger than in our models (1.6 nm). The experimentally observed energy difference ranges from 50 to 20 meV [16] and is an order of magnitude lower than the one from the DFT calculation. Thus, a direct assignment of the calculated splitting to the experimental results is not possible, maybe due to a different edge chemistry, but our findings suggest that the interpretation of a double peak around E_F alone as a sign for edge magnetism might be misleading.

The electronic structure of H-free GNRs on Ag(111) is qualitatively similar to that of the nanoribbons deposited on Au, as discussed in the Supplemental Material [32]. On the other hand, H-terminated GNRs on Ag(111) exhibit remarkable differences with respect to Au(111), which originate from the relatively stronger interaction between

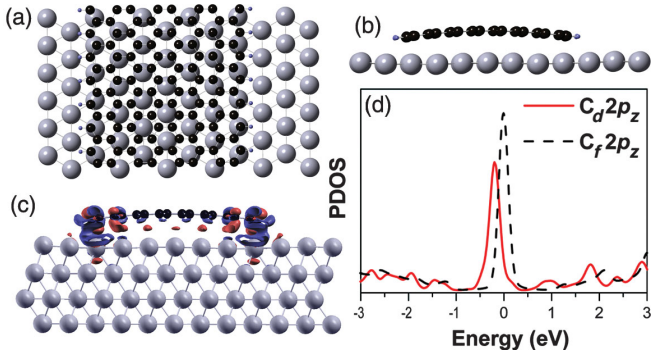

FIG. 3 (color). Structural and electronic properties of a H-terminated GNR on Ag(111). (a), (b) Top and side view of the relaxed model. Only the top Ag layer is shown. (c) Isovalue surfaces of the difference between the total charge of the GNR plus substrate system and the charge of the isolated (bent) GNR and Ag(111). The red (blue) color indicates accumulation (depletion) of charge. (d) PDOS of the $2p_z$ orbitals of an edge C atom of the deposited GNR (C_d). The non-spin-polarized $2p_z$ PDOS of the edge C atom of the free-standing GNR (C_F) is also shown.

the edges of the GNRs and the Ag substrate. This fact is probably due to the less diffuse character of the 4d orbitals of Ag as compared to the 5*d* orbitals of Au. The minimum distance between the C atoms and Ag(111) is 2.69 Å at the edge (Table I) and a more significant bending of the GNR occurs [Figs. 3(a) and 3(b)]. As a result of the chemical interaction between Ag(111) and the GNR, a significant charge rearrangement also occurs at the interface, as evident from Fig. 3(c). In total, the GNR has acquired a charge of 1.6×10^{-2} electrons per C atom (corresponding to 0.13 electrons per edge C atom). This behavior is in contrast to the case of Au(111), where doping is essentially negligible. The doping of perfect monolayer graphene has also been shown to depend sensitively on the type of metal substrate, even in the weak bonding case [38–41] (see also the discussion in the Supplemental Material [32]). The PDOS of the C $2p_z$ orbitals exhibits a large peak [Fig. 3(d)], which corresponds to the edge states. However, due to the *n* doping of the GNR, the peak is not exactly at E_F but is shifted slightly downwards in energy. Furthermore, the height of the PDOS peak is reduced with respect to the free-standing case, due to the interaction with the Ag atoms [Fig. 3(d)]. As a result, no Stoner instability occurs: hence, this system is nonmagnetic. In fact, the calculated magnetization is less than $10^{-3}\mu_B$ per edge C atom. Notice that, in the case of free-standing GNRs, a larger doping density is needed to fully destroy edge magnetism [20,21,42]. Therefore, the absence of magnetism in our model is due to a subtle interplay between charge transfer and the chemical interaction with the substrate.

GNRs on Cu(111) display significant structural differences with respect to the Au and Ag substrate (see Supplemental Material [32]). In the H-free case, the edge state interacts more strongly with the Cu substrate than with Au(111) and Ag(111): nevertheless, the PDOS bears a qualitative resemblance to that of the latter models. Furthermore, the interaction between the GNR and the Cu substrate is not negligible even in the center of the GNR and the maximum distance between the latter and the surface is only 3.31 Å (see Table I and Fig. S2a): the latter property, however, might be due to the use of a compressed surface or to the van der Waals coefficients employed for Cu (see Supplemental Material [32]) and requires further investigation. In the H-terminated case, the relatively strong interaction between C and Cu atoms also leads to shorter equilibrium distances between the GNR and the substrate [Table I and Figs. S5(a)–(b)]. N doping leads to the filling of the edge state in this model too, which is also nonmagnetic [Figs. S5(c)–(d)].

In conclusion, our simulations based on DFT indicate that zigzag GNRs deposited on Cu(111), Ag(111), and Au(111) all possess edge states but do not exhibit significant edge magnetism, with the exception of H-terminated GNRs on Au(111), whose zero-temperature magnetization is comparable to that of free-standing GNRs. These results are explained by the different interaction and charge transfer between the GNRs and the substrates and show that edge magnetism in zigzag GNRs can be destroyed even upon deposition on a substrate which interacts weakly with graphene. Only in the case of H-terminated GNRs on Au(111) is the interaction at the edge sufficiently weak so as not to affect the electronic and magnetic properties of the edge states significantly. Hence, our simulations strongly suggest that experimental investigations on edge magnetism in GNRs deposited on metallic substrates should focus on the latter system.

We acknowledge discussions with G. Bihlmayer, C. Honerkamp, M. Schmidt, and S. Wessel, the computational resources by the RWTH Rechenzentrum, as well as financial support by DAAD and DFG via Li 1050/2-1 and Mo 858/8-2.

*mazzarello@physik.rwth-aachen.de

[1] A. H. C. Neto, F. Guinea, N. M. R. Peres, K. S. Novoselov, and A. K. Geim, Rev. Mod. Phys. **81**, 109 (2009).
[2] S. V. Morozov, K. S. Novoselov, M. I. Katsnelson, F. Schedin, D. C. Elias, J. A. Jaszczak, and A. K. Geim, Phys. Rev. Lett. **100**, 016602 (2008).
[3] P. J. Zomer, S. P. Dash, N. Tombros, and B. J. van Wees, Appl. Phys. Lett. **99**, 232104 (2011).
[4] Y. Son, M. L. Cohen, and S. G. Louie, Nature (London) **444**, 347 (2006).
[5] L. Jiao, L. Zhang, X. Wang, G. Diankov, and H. Dai, Nature (London) **458**, 877 (2009).
[6] J. Cai *et al.*, Nature (London) **466**, 470 (2010).
[7] X. Li, X. Wang, L. Zhang, S. Lee, and H. Dai, Science **319**, 1229 (2008).
[8] L. A. Ponamarenko, F. Schedin, M. I. Katsnelson, R. Yang, E. W. Hill, K. S. Novoselov, and A. K. Geim, Science **320**, 356 (2008).

[9] F. Molitor, S. Dröscher, J. Güttinger, A. Jacobsen, C. Stampfer, T. Ihn, and K. Ensslin, Appl. Phys. Lett. **94**, 222107 (2009).
[10] K. A. Ritter and J. W. Lyding, Nat. Mater. **8**, 235 (2009).
[11] M. Fujita, K. Wakabayashi, K. Nakada, and K. Kusakabe, J. Phys. Soc. Jpn. **65**, 1920 (1996).
[12] K. Nakada, M. Fujita, G. Dresselhaus, and M. S. Dresselhaus, Phys. Rev. B **54**, 17 954 (1996).
[13] T. Wassmann, A. P. Seitsonen, A. M. Saitta, M. Lazzeri, and F. Mauri, J. Am. Chem. Soc. **132**, 3440 (2010).
[14] Z. Klusek, W. Kozlowski, Z. Waqar, S. Datta, J. S. Burnell-Gray, I. V. Makarenko, N. R. Gall, E. V. Rutkov, A. Ya. Tontegode, and A. N. Titkov, Appl. Surf. Sci. **252**, 1221 (2005).
[15] M. Pan, E. C. Girao, X. Jia, S. Bhaviripudi, Q. Li, J. Kong, V. Meunier, and M. S. Dresselhaus, Nano Lett. **12**, 1928 (2012).
[16] C. Tao *et al.*, Nat. Phys. **7**, 616 (2011).
[17] J. Chae, S. Jung, S. Woo, H. Baek, J. Ha, Y. J. Song, Y.-W. Son, N. B. Zhitenev, J. A. Stroscio, and Y. Kuk, Nano Lett. **12**, 1839 (2012).
[18] W. Y. Kim and K. S. Kim, Nat. Nanotechnol. **3**, 408 (2008).
[19] K. Wakabayashi, Phys. Rev. B **64**, 125428 (2001).
[20] M. Wimmer, I. Adagideli, S. Berber, D. Tománek, and K. Richter, Phys. Rev. Lett. **100**, 177207 (2008).
[21] J. Kunstmann, C. Özdoğan, A. Quandt, and H. Fehske, Phys. Rev. B **83**, 045414 (2011).
[22] D. Subramaniam *et al.*, Phys. Rev. Lett. **108**, 046801 (2012).
[23] P. Lacovig, M. Pozzo, D. Alfè, P. Vilmercati, A. Baraldi, and S. Lizzit, Phys. Rev. Lett. **103**, 166101 (2009).
[24] S. K. Hämäläinen, Z. Sun, M. P. Boneschanscher, A. Uppstu, M. Ijäs, A. Harju, D. Vanmaekelbergh, and P. Liljeroth, Phys. Rev. Lett. **107**, 236803 (2011).
[25] S.-H. Phark, J. Borme, A. L. Vanegas, M. Corbetta, D. Sander, and J. Kirschner, Phys. Rev. B **86**, 045442 (2012).
[26] S. J. Altenburg, J. Kröger, T. O. Wehling, B. Sachs, A. I. Lichtenstein, and R. Berndt, Phys. Rev. Lett. **108**, 206805 (2012).
[27] I. Pletikosić, M. Kralj, P. Pervan, R. Brako, J. Coraux, A. T. N'Diaye, C. Busse, and T. Michely, Phys. Rev. Lett. **102**, 056808 (2009).
[28] C. Busse *et al.*, Phys. Rev. Lett. **107**, 036101 (2011).
[29] Y. Li *et al.*, Adv. Mater. **25**, 1967 (2013).
[30] L. Y. Jiao, X. R. Wang, G. Dyankov, H. L. Wang, and H. Y. Dai, Nat. Nanotechnol. **5**, 321 (2010).
[31] H. Feldner, Z. Y. Meng, T. C. Lang, F. F. Assaad, S. Wessel, and A. Honecker, Phys. Rev. Lett. **106**, 226401 (2011).
[32] See Supplemental Material at http://link.aps.org/supplemental/10.1103/PhysRevLett.110.216804 for additional computational details, the description and discussion of further models of graphene and GNRs on Cu, Ag and Au and a further analysis of a) doping effects due to the substrates and b) chemical interaction at the edge.
[33] P. Giannozzi *et al.*, J. Phys. Condens. Matter **21**, 395502 (2009); http://www.quantum-espresso.org.
[34] J. P. Perdew, K. Burke, and M. Ernzerhof, Phys. Rev. Lett. **77**, 3865 (1996).
[35] S. Grimme, J. Comput. Chem. **27**, 1787 (2006).
[36] X. Zhang *et al.*, ACS Nano **7**, 198 (2013).
[37] L. Talirz *et al.*, J. Am. Chem. Soc. **135**, 2060 (2013).
[38] G. Giovannetti, P. A. Khomyakov, G. Brocks, V. M. Karpan, J. van den Brink, and P. J. Kelly, Phys. Rev. Lett. **101**, 026803 (2008).
[39] M. Vanin, J. J. Mortensen, A. K. Kelkkanen, J. M. Garcia-Lastra, K. S. Thygesen, and K. W. Jacobsen, Phys. Rev. B **81**, 081408 (2010).
[40] J. Sławińska, P. Dabrowski, and I. Zasada, Phys. Rev. B **83**, 245429 (2011).
[41] J. Gebhardt, F. Viñes, and A. Görling, Phys. Rev. B **86**, 195431 (2012).
[42] J. Jung and A. H. MacDonald, Phys. Rev. B **79**, 235433 (2009).